COMBUSTION EXPERIMENTS ON THE MIR SPACE STATION

Paul Ferkul*, Kurt R. Sacksteder†, Paul S. Greenberg† Daniel L. Dietrich†, Howard D. Ross†, James S. T'ien‡, Robert A. Altenkirch§, Lin Tang§, Matt Bundy¶, and Michael Delichatsios#

Abstract

Combustion tests were carried out on the Mir Space Station. Flat sheets of paper, polyethylene-insulated wires, cylindrical cellulosic samples, and candles were burned in microgravity. The test parameters included sample size, fuel preheating levels, and low-speed air velocity.

Data were collected mainly through video cameras, audio recordings of crew observations, and 35 mm still pictures. For many of these tests, thermocouples permitted the recording of temperatures of the gas phase flame and/or solid fuel. After the flight, the flame images and temperature data were compared to numerical simulations.

Several unique phenomena were observed and the results have implications for spacecraft fire safety. These include the influence of airflow, fuel melting and bubbling, and fuel-vapor generation, and condensation after the flame extinguished.

Introduction

In recent years, the number of combustion experiments utilizing a microgravity (or "weightless") environment has increased dramatically. While performing such experiments continues to be challenging, the resulting data are unique and easier to model, and relate directly to terrestrial or space-based applications.

For most flames burning on Earth, the effect of gravity is dramatically manifested: hot air produced by the flame tends to rise because of buoyancy. This creates flow effects that can complicate or completely mask elements essential to understanding the combustion process.

A number of reviews examine the role of buoyancy in combustion. Law[1] discusses opportunities provided by a microgravity environment for fundamental combustion research, reports on progress in microgravity combustion research, and emphasizes the potential of fire hazards in space and the challenges to devise rational fire prevention strategies. He places such studies in the larger context of unsolved or emerging combustion-dominated problems, including energy conservation, air pollution, surface transportation, aeropropulsion, hazardous waste incineration, materials processing, and global warming.

Williams[2] presents the conservation equations of combustion, with relevant nondimensional parameters identified, for focusing on the role of buoyancy. His objective is to indicate ways that microgravity combustion experiments can be devised to investigate certain aspects of chemically reacting flows not readily studied in normal gravity. Potential areas for advances in understanding combustion through microgravity experiments are listed.

Faeth[3] reviews gaseous flame research as it relates to microgravity. He lists two major findings: First, that only experiments in microgravity can resolve many fundamental issues of combustion science; and second, that flame processes at microgravity and normal gravity are usually very different. These findings both justify studying flames in microgravity, and raise concern about the relevance of earth-based fire-safety technology to spacecraft environments.

More recently, King and Ross[4] discuss the importance of microgravity to the study of fundamental combustion phenomena and present an overview of the

*National Center for Microgravity Research, Senior Member
† NASA Lewis Research Center
‡ Case Western Reserve University
§ Mississippi State University
¶ Washington State University
# Renewable Resources Associates

past and current NASA microgravity combustion program.

Ross[5], who documents the accidental fire aboard the Mir Space Station in February, 1997, further reinforces the need for microgravity combustion experiments from a different viewpoint. This event is a reminder of the importance of understanding fire characteristics, detection, and suppression in microgravity. Not only are huge investments in capital equipment at risk, but so are the lives of people in the extreme and hostile environment of outer space. Ross makes the further link to the on going and planned mission to Mars, which presents even larger challenges and perils than mere Earth orbit.

This paper presents results from three combustion science experiments that were conducted aboard the Mir Space Station. Each of them have been described more fully in other documents, and are described here collectively to demonstrate trends related to fire spread in microgravity.

The Forced Flow Flame spreading Test (FFFT)[6] examined the combustion of thin cellulosic sheets of fuel and electrically heated polyethylene cylinders. The Opposed Flow Flame Spread (OFFS) experiment[7] investigated the combustion of cylinders of paper. Finally, the Candle Flames in Microgravity (CFM) experiment[8] studied the behavior of candles in different configurations. While providing fundamental scientific data, these experiments have direct application to understanding the combustion phenomena that underlie the engineering of fire prevention, detection, and suppression practices.

The Mir fire incident mentioned above occurred during the mission on which one of these experiments was performed. Astronaut Jerry Linenger described his experience with the OFFS tests in the context of the potentially life-threatening fire from the solid oxygen canister:

> "The biggest joy is conducting good experiments, and I had some very interesting things. One is looking in a glovebox at flame propagation, and after the fire, after seeing the real thing and then being able to experiment, change ventilation rates, things like that, it was very interesting."[9]

A direct application of microgravity combustion experiments is spacecraft fire safety, and the Mir fire underscores this connection.

Hardware Description

MirGBX The three experiments were conducted inside the Microgravity Glovebox (MirGBX). The MirGBX provides an ergonomical and sealed working volume designed to handle biological, fluids, combustion, and materials experiments that might involve small quantities of potentially hazardous substances. As an experiment platform, the MirGBX provides power, cooling, film and video imaging capabilities, isolation from cabin lighting, and a level of containment for the combustion products. The MirGBX is a multi-user facility developed by the European Space Agency/ESTEC with Brunel Institute for Bioengineering (United Kingdom), and Bradford Engineering (the Netherlands) under contract with Teledyne Brown Engineering for the NASA Marshall Space Flight Center.

The three combustion experiment payloads described here were all built specifically for operation in the MirGBX by the NASA Lewis Research Center.

FFFT The hardware consisted of a test module, which was a miniature, low-speed wind tunnel; a hand-held control box; and a set of eight fuel sample assemblies (fig. 1). The test module was a metallic duct with an inlet section, where air velocity measurements were made, and an outlet section where the fan that moves the air was located. The test section in the middle was isolated from the inlet and outlet sections by small mesh screens that conditioned the air flow, absorbed the heat of the flame, and prevented the escape of any particulates (like soot) created during the burning.

The front of the test module was a window that opened to provide access for installing and removing fuel samples. An additional fixed window was located on the top of the duct. Thermocouples located near and inside each fuel sample provided measurements of both fuel and flame temperatures. The temperature values were presented on digital displays in the front window of the test module.

A video camera simultaneously imaged the flame, the six thermocouple displays, and an air velocity or anemometer display by viewing the front window of the module. A 35mm camera provided high-resolution still images of the flame through the top window of the module.

Eight fuel samples of two different types were flown. The first four samples were flat paper (cellulose)

sheets of different thicknesses lying in a plane parallel to the flow; the remaining four samples were 1.5-mm diameter cylinders of polyethylene formed around an inert core that could be heated electrically (conventional electrical wire insulation). The axes of the cylinders were aligned with the flow direction. Ignition was achieved using a separate electrically heated wire.

The flat samples provide a two-dimensional geometry in rectangular coordinates for ease of modeling. Cylindrical samples were chosen because their axi-symmetry is also more easily modeled. In addition, the cylindrical samples resemble electric cables, which may be involved in the most likely spacecraft fire scenario.

The test module was operated using the control box, located outside the MirGBX and linked to the test module through a connector in the MirGBX front door. The cellulose tests were conducted in approximately 21-23% oxygen, the polyethylene in approximately 25% oxygen.

OFFS The experiment utilized two slightly-modified FFFT test modules (one each for low-speed and high-speed flow) as described above, along with different fuel samples (fig. 2). This hardware flew previously aboard the Space Shuttle during STS-75. The main difference with the FFFT hardware was the installation of an improved fan control circuit, and the replacement of one of the thermocouple displays with a fan speed indicator.

All OFFS fuel samples were paper (cellulose) formed into cylinders of different inner and outer diameters. Three were 7 mm outer diameter, and were mounted on ceramic cores 3 mm in diameter, for a wall thickness of approximately 2 mm. Three were 12 mm outer diameter which were solid at one end and hollow at the other, on 8 mm diameter cores for a 2 mm wall thickness again (the igniter was located at the hollow end). The remaining two samples were 12 mm diameter and were solid. Oxygen concentrations were between 20-23% at the time of testing.

CFM The design of the Candle Flames in Microgravity Experiment was based on the earlier experiment conducted aboard the Space Shuttle USML-1 mission and described in detail elsewhere[10]. The main module (fig. 3) of the experiment was a 20 cm cube-shaped wire mesh screen (as opposed to the 12.5 cm perforated Lexan box used on USML-1). The screen provided more than 50% free area (this was less than 15% on USML-1) yielding less resistance for oxygen to diffuse to the flame and combustion products to diffuse away from the flame.

Thermocouples provided gas phase temperature data, and a radiometer measured incident radiation from the candle flame. A single point oxygen sensor was installed to provide a record of the local oxygen concentration.

The ignition system was a coiled 250 μm aluminum alloy wire heated with a current of approximately 3 amperes. For all of the experiments, the igniter was on for a preset time of 4 or 5 seconds. This was sufficient to ignite the candle in almost all of the tests.

A variety of candle types were flown. There were 79 total candles supplied with the hardware with three different wick diameters (approximately 1, 2 and 3 mm), two different candle diameters (5 and 10 mm) and two different lengths of initially exposed wick (3 and 6 mm). All candles were 2 cm in length. Oxygen concentrations were 22-25% at the time of testing.

Results

Paper Sheets (FFFT) The effect of varying fuel thickness at a constant flow speed of 2 cm/s was examined for four different samples, having area densities (mass density times half-thickness) of 1.0, 4.0, 16, and 40 mg/cm^2.

Typical flame images are shown for each test in fig. 4. The fuel is viewed edge on, so the left and right flame halves enclose the fuel symmetrically. The samples are ignited at the bottom and the flow direction is from bottom to top, yielding the concurrent-flow configuration. (In some cases, glowing thermocouple leads can be seen.)

Note that the flames are wide, dim, and mostly blue. The wide flames are due to small airflow speed, and the dim blue flame is due to slow oxygen transport. The second sample burned anomolously because it was manipulated after a failed first ignition attempt. Failure of the second sample to ignite before the airflow was initiated indicates the necessity of flow for material flammability in that atmosphere.

In normal-gravity upward burning of paper, higher speed buoyant flow provides oxygen sufficient to support plentiful soot production with narrow, bright,

yellow flames. Higher flow velocities cause the flames to accelerate continually, becoming long and turbulent.

Fig. 4 also shows approximate flame propagation rates of the FFFT samples. The disappearance of the fuel leading edge, termed the flame base spread rate, varies inversely with fuel thickness, consistent with theoretical predictions. Because of the constant ignition power used for each sample, the initial flame lengths shrank for the thinner samples and grew for the thicker samples.

Temperature traces for one case are shown in fig. 5. Three of the thermocouples were initially mounted on the solid fuel. These indicated temperatures show the fuel heat up, plateau while the fuel undergoes pyrolysis and vaporization, then rise to flame temperatures after the fuel disappears and the flame passes. The relatively cool peak flame temperatures (compared to normal gravity) are consistent with the flame's dim, blue color and are too low to encourage soot production.

Polyethylene Cylinders The polyethylene cylinders were heated to between 85 and 100 C prior to ignition by resistance heating the wire core. Two of the cylinders were ignited in a concurrent flow, the other two in opposed flow.

Figure 6 shows two sequences of images from the polyethylene samples. As the flames spread, the fuel melts and flows into a transparent ellipsoidal bead. In each case, the molten fuel bead grows during flame spreading and remains inside the flame. As the beads of molten fuel grow, fuel vapor bubbles gradually form then burst, releasing small jets of fuel vapor that briefly distort the flame (seen in the images as a random fluctuation in the flame shape). Bursting bubbles also eject small flaming particles that are carried downstream. When the flames reach the end of the fuel sample, the flame behavior is completely dominated by the formation and bursting of fuel vapor bubbles. In each case, the fuel is completely consumed by the flame. In normal gravity tests, melting fuel flows or drips downward, exiting the flame zone.

In contrast to the cellulose samples, soot was emitted from the flames in very long or continuous agglomerate threads. Earlier tests of this type conducted aboard the Space Shuttle[11] showed similar long threads and primary particles slightly larger than soot primaries collected from identical samples in normal gravity.

Normal gravity flame spread behavior of identical fuel samples is quite different than the FFFT results. In addition to the removal of significant fuel from the flame by dripping, buoyant airflow carries soot quickly through the flame, preventing the extended growth of soot agglomerates.

Table 1 shows a summary of the flame-spread rates of the polyethylene samples. The spread rates increase with increasing airflow velocity, consistent with predictions in low speed flows. Additionally, the spread rates are higher for concurrent flow than for opposed flow at comparable airflow velocity.

Table I. FFFT Polyethylene sample flow conditions and spread rates in 25% oxygen.

Test	Flow Speed (cm/s) and direction	Flame Base Spread Rate (cm/s)
1 (Mir)	2 (Concurrent)	0.16
2 (Mir)	3 (Opposed)	0.12
3 (Mir)	1 (Concurrent)	0.15
4 (Mir)	1 (Opposed)	0.11

Paper Cylinders (OFFS) The samples and igniters were arranged to yield opposed-flow flames. Contrary to the polyethylene cylinder tests, these samples were not preheated. Therefore, a substantial amount of energy released by the flame was used to heat the fuel core as the flame spread.

Of the eight samples that were flown, four could be ignited: all three of the samples with the small diameter, and one of the larger samples. The remaining large samples could not be ignited. Possible explanations include a reduced cabin oxygen concentration being too low (about 20%) compared to earlier tests, and the possibility that radiative losses from the fuel surface (area) and flame (volume) increase sufficiently with sample radius to render the sample not flammable.

In fig. 7, the evolution of two of the flames over the smaller cylinders is shown as a function of time. As with the paper sheets, the flames are dim and blue. The spread rate more than doubles as the flow speed is increased from 3 to 5 cm/s. This is completely different from the trend in normal gravity where increasing the airflow may *decrease* the spread rate,[12] and suggests the importance of the flow to the material flammability.

The only large diameter sample that was burned had a partially hollow core, as described earlier. The intention of this test to to seek a flow velocity at which the air flow was insufficient to sustain the flame. The sample was ignited at a relatively high flow velocity (9 cm/s), but as hoped the flame went out as the velocity was subsequently reduced to approximately 5 cm/sec.

Candles Unlike the flames presented earlier, the candle flames had no airflow imposed on them and so were exceptionally dim. The MirGBX color video cameras lacked sufficient low-light sensitivity to adequately image them. Additionally, a concern about film fogging (owed to long-term exposure to cosmic radiation while in space) precluded the use of high-speed 35 mm film. The ASA 200 film that was used resulted in very long open-shutter times. The combination of imaging system weaknesses reinforced the critical importance of astronaut observations in describing the processes.

Qualitatively, all of the candles burned similarly in the following ways. Immediately after ignition, the flames were very luminous and near spherical to hemispherical. As the burning progressed, heat feedback from the flame rapidly melted the wax. For the 5 mm diameter candles, all of the exposed wax melted within 2 minutes of ignition. In comparison, the exposed wax melts in about 10 minutes in normal gravity. The shape of the candle and wax then looked as in fig. 8(b). After some time, this molten ball of wax became unstable and 'collapsed' suddenly as it moved back along the candle holder as shown in fig. 8(c). After the collapse, the yellow luminosity disappeared and the flame became and remained dim blue until extinction.

The flame lifetimes varied from slightly over 100 seconds to over 45 minutes. The candles with the largest wicks had the shortest flame lifetimes and the candles with the smallest wicks had the longest flame lifetimes. The actual flame lifetime for seemingly identical candles varied significantly in some cases.

The spontaneous, pre-extinction flame oscillations (observed to last only a few seconds in the USML-1 tests[10]) also occurred with the Mir flames, and persisted up to 90 sec for the two larger wick diameters. (Oscillations could only be *induced* in the experiments with the smallest wick diameter while the thermocouple was positioned close to the flame.)

Figure 9 shows flame dimensions (as defined in fig. 8a) as a function of time for a typical Mir candle flame with a relatively long lifetime. The flame size increases for the first 75 sec of the flame lifetime, after which the flame size remains relatively constant (D remains constant, but H decreases slowly). This change in behavior at 75 seconds corresponds to the time of the collapse of the liquid wax. H/D is nearly steady until the collapse occurs after which it continuously decreases until extinction.

Figure 10 shows the flame diameter (D) as a function of time for the three different wick sizes. As expected the larger the wick size, the larger the quasi-steady flame size. The mass burning rate of the candle flame should also be a function of the candle wick diameter. The three different wick sizes give burning rates that varied from 0.9 to 1.4 mg/s in normal gravity. The reduced gravity burning rates (based on the candle mass before and after the experiments) varied from approximately 0.2 mg/s for the smallest wick size to 0.6 mg/s for the largest.

With the MirGBX working lights on, it could be seen that there was a significant amount of aerosol produced at the base of the flame near the candle holder. The aerosol was in all likelihood condensed paraffin produced from the flame vaporizing the wax. It moved along the candle, exited the flame (perhaps carried in the boundary layer produced by the liquid wax flow), and condensed as it get far enough away. Throughout the lifetime of the flame, aerosol streamed out from the base of the candle and formed a ring around the inside of the candle box. This last observation was not evident on the video camera, but described in detail by the crew. After flame extinction, there was also a large, spherical vapor cloud that surrounded the candle and was centered at the wick.

Modeling The numerical models for these flame systems are described in detail elsewhere.[14,15,16] Selected comparisons of these models with experiment are presented here. Fuel consumption rate contours are compared directly to the flame. These contours are the best indicator of the blue visible flame in models with one-step kinetics. In order to achieve the best agreement with experimental data, Grayson et al.[13] used w_F= 0.1 mg/s cm^3 to represent the edge of the blue flame (minimum visible reaction rate) in related solid-fuel flame-spread modeling, and the same value is used here.

In modeling the candle flames, comparison between the computed flame shape and the experimen-

tal photographs shows good agreement[16]. However, the numerical model produces a more hooked base than was present in the experiment, probably due to the assumption that the fuel source in the model is a sphere, whereas experimentally it is more cylindrical (see fig. 8(a) for a depiction of the model geometry).

A sample of the results is shown in fig. 11(a) at 0.23 mole fraction oxygen ambient. (Only one-half of the picture is shown because of symmetry.) The computed peak temperature is around 1710 K and a cool zone exists near the wick (or cold rod). Figure 11(b) shows the fuel-vapor mass-fraction contours. Some fuel vapor leaks out from the inside of the flame because of the quench layer near the wick. Similarly oxygen, shown in fig. 11(c), diffuses through this cool zone into the fuel-rich zone between the flame and the wick, thus creating a small partially premixed region. Figure 11(d) is a plot of the fuel vapor reaction (consumption) rate contours. Figure 11(d) clearly shows a quench zone near the wick. (This zone provided a path for the aerosol to stream out of the flame, as described earlier.)

In recent preliminary work, the near-limit flame oscillations observed experimentally have been simulated numerically. The frequency is similar to that observed experimentally (but at a much smaller amplitude), and the nature of the oscillation is similar[16].

The computed flame[14] for combustion of the thin paper sheet of FFFT sample 1 is shown in fig. 12. The curvature of the visible flame is in good agreement with that of the computed reaction rate contour. The visible flame is longer than predicted, however, but note that the flame is shrinking throughout the test time. The model also predicts a spread rate of 0.59 cm/sec compared to the measured value of the flame tip propagation of 0.58 cm/sec. The predicted peak temperature of 1345 deg. C is compared to the measured value of 1177 deg. C from uncorrected thermocouple signals. These comparisons show good agreement, even though the computed flame is steady while the observed flame is shrinking.

Importance of Air Flow Air motion (or lack of it) is an important factor in determining flame characteristics and material flammability[17,18,19]. In normal gravity, buoyancy forces prevent the study of low-speed airflow on flames. However, in microgravity, zero-speed or very low-speed forced flows provide access to test regimes where other mechanisms, such as radiation heat transfer, control flame characteristics. By exploiting the unique flow environment afforded by microgravity, and together with modeling results, these experiments have provided insight into the underlying physics of combustion of solid materials.

The transfer of oxygen to the flame is crucial in determining its strength and viability. The candle flames, which were in quiescent environments, relied solely upon diffusion and "self-generated" flow (aerosol streaming description earlier, e.g.) for transport of its reactants. While the flames were quite weak, as evidenced by the fact that the video cameras could not image them, they persisted for a very long time, in fact longer than in normal gravity.

The fact that a flame can be established in a quiescent environment has implications for fire safety. Clearly, sometimes it may not be adequate to merely turn off the air circulation to extinguish a fire in a spacecraft. More localized detection and active extinguishment would be needed in such cases. In addition, smoke detectors would be unable to sense these kinds of weak, non-smoking flames. This failure may often be moot, as the invisible flames would likely be too weak to spread or ignite surrounding material.

In the experiments examining the combustion of solid sheets and cylinders, there is always a slow flow of air supplied to the flame. The effect of the flow is dramatically seen as small changes lead to significant variations in flame size and spread rate.

Liquid Fuel Effects The polyethylene cylinders and candles produced molten fuel, which in turn led to significant fluid-mechanical effects. In these tests, the flame developed, and eventually melted all the remaining fuel in an increasingly large molten mass held together by surface tension. The liquid fuel acted as a large stable reservoir feeding the flame for a very long time.

In normal gravity upward and horizontal burning tests, the fuel tended to drip off and not be consumed. Absent this effect, the *total* amount of heat (and product gases) released in microgravity can be larger, even though the rate of fuel consumption is smaller. Therefore, for fuels that melt, relying on a normal gravity assessment for the microgravity fire hazard can be quite misleading.

The generation of the wax vapor (or aerosol) observed for the candles implies that a significant amount of fuel escapes the flame. This is possible between the wick and the flame, where the quench zone

provides the path for mass transfer to the surroundings (also suggested by the model). The fuel-rich gas in this region is pumped out of the flame by the thermocapillary flow in the molten mass of wax, which tends to move from the tip of the wick down and away from the flame. Given the long burning times of the candles, even a slow accumulation rate of aerosol mist will eventually lead to an observable concentration (note that there is no sedimentation in microgravity).

Furthermore, when astronaut Dr. Shannon Lucid switched the chamber lights on after the candle flame extinguished, the biggest surprise was the appearance of a white ball surrounding the candle tip[20]. The ball is believed to be a fog of droplets that formed after flame extinction, when wax vapor still issuing from the hot wick condensed in the colder air. The formation of this flammable cloud served as an excellent reminder regarding fire safety in spacecraft: the hazardous event is not ended when the fire extinguishes because flammable material can continue for some time to issue from the source of the fire.

Ejection of particles due to fuel boiling/bubbling is a hazard for space fire, and has been suggested elsewhere[21,22]. In burning the polyethylene cylinders, small bubbles of gas form in the liquid mass and are periodically ejected from the flame. This bubbling and sputtering type of behavior intensified as the burns progressed (probably due to the liquid heating up). In microgravity, these flaming ejecta can travel far, providing ignition sources. NASA's flammability test (Test 1 of NHB8060.1C[23]) takes account of this phenomenon when determining the acceptability of a material for use in spacecraft.

Modeling Implications Model predictions are close to experimentally measured flame shapes and temperatures. Through parametric studies, the models have shown the importance of gas and surface radiation in controlling flammability and extinction. Thus the weak flames observed can be controlled by radiative processes. The data provided by these experiments have made clear the need for detailed consideration of radiation from microgravity flames, which is of growing interest.

For the candle flames, spontaneous flame oscillations are inherent to their near-extinction behavior. The observed frequency was consistent with those seen before in low gravity, and are much less than observed in normal gravity[10]. The apparent dependence on wick diameter, implying a dependence on flame size, suggests that flame radiative losses may contribute to the onset of oscillations, as hypothesized by Cheatham and Matalon[24]. Microgravity tests have enabled this observation of the important radiative effects, otherwise masked by buoyancy.

Glovebox Limitations While the MirGBX provided a convenient platform for performing small-scale combustion experiments, limitations were evident. For the thin sheets of cellulose, the fact that the flames had not reached a steady size during their development and spread suggests that a longer sample is required than can be accommodated in this facility. Modeling results indicate that a steady state does exist, but because of the size limitations, was not observed in the experiment.

For the candle experiments, both the oxygen sensor and radiometer data lacked sufficient resolution, since the MirGBX data recorder provided only six-bit digitization (eight-bit performance was anticipated).

The exact value of the local atmospheric oxygen content in the glovebox at the time of the combustion tests was close to cabin air, which itself was not exactly known (it varied between 20% and 25% O_2). Specifically, for the cellulose cylinders that could not be ignited, it is possible that the oxygen content was too low compared to the other (earlier) successful tests.

Concluding Remarks

In the range of low-speed flows tested, increasing the flow rate caused the flames to strengthen significantly (see fig. 7, e.g.). When the forced air flow was stopped, the flames self-extinguished. In contrast, the candle flames persisted in a quiescent environment. Similar to candles, droplet combustion persists in quiescent environments, as do other combustion systems[5]. While extinguishment in space is certainly promoted when ventilation is stopped, it is not always certain that this method will be 100% effective in isolation. Thus active fire extinguishers are necessary to be incorporated into a complete fire safety strategy for spacecraft.

The candle flames obtained were quasi-steady (and lasted up to 45 minutes), meaning that the flame was steady over a time period much longer than any reasonable characteristic gas-phase transport time. These experiments however were conducted in the somewhat enriched oxygen atmosphere of the Mir, so it remains debatable whether they would persist in air.

The microgravity experiments provided evidence of the importance of radiation for controlling these flames. This observation has been suggested by the modeling effort, and is applicable only when the complicating effects of buoyancy are not present.

Low-speed air flow, 'self-generated' gas flow, molten fuel effects, large scale thermocapillary effects, vapor 'cloud' generation, and flaming ejected particles were described. These all have important application to spacecraft fire safety, and demonstrate the need to analyze flammability risks on a case-by-case basis.

Acknowledgments

We would like to gratefully acknowledge the work of Richard Pettegrew and Nancy Piltch in conducting ground tests, preparing the hardware for flight, and assisting with data analysis. In addition, we thank astronauts Shannon Lucid and Jerry Linenger who not only conducted the experiments, but provided important verbal observations recorded during the tests.

References

[1]Law, C. K.: Combustion in Microgravity: Opportunities, Challenges, and Progress, AIAA 28th Aerospace Sciences Meeting, AIAA-90-0120 (1990).

[2]Williams, F. A.: Combustion Phenomena in Relationship to Microgravity Research, Microgravity Science and Technology III, No. 3, pp. 154-161 (1990).

[3]Faeth, G. M.: Homogeneous Premixed and Nonpremixed Flames in Microgravity: A Review, Proceedings of the AIAA/IKI Microgravity Science Symposium, pp. 281-293 (1991).

[4]King, M. K. and Ross, H. D.: Overview of the NASA Microgravity Combustion Program, AIAA Journal, Vol. 36, No. 8, pp. 1337-1345 (1998).

[5]Ross, H. D.: Burning To Go: Combustion On Orbit and Mars, Fall Technical Meeting of the Eastern States Section of the Combustion Institute (1997).

[6]Sacksteder, K.R., T'ien, J.S., Greenberg, P.S., Ferkul, P.V., Pettegrew, R.D., and Shih, H.Y., "Forced Flow Flame Spreading Test: Findings from the Shuttle/Mir Phase-1 Mission, Increment Two," submitted to NASA JSC Mission Science, (1998).

[7]Opposed Flow Flame Spread on Cylindrical Surfaces (OFFS), 1-year report, NASA Johnson Space Flight Center (1998).

[8]Dietrich, D. L., Ross, H. D., and T'ien, J. S.: Candle Flames in Microgravity-2 (CFM-2), Science Requirements Document, Microgravity Science Division, NASA Lewis Research Center (1998).

[9]From a transcription of the post-mission press conference held by Jerry Linenger (1997).

[10]Dietrich, D. L., Ross, H. D. and T'ien, J. S.: Candle Flames in Weakly-Buoyant and Non-Buoyant Atmospheres, AIAA-94-0429 (1994).

[11]Greenberg, P.S., Sacksteder, K.R., Kashiwagi, T., "Wire Insulation Flammability Experiment: USML-1 One Year Post Mission Summary," NASA CP 3272, Vol II, pp. 631-656, (1994).

[12]Fernandez-Pello, A. C., Ray, S. R., and Glassman, I.: Flame Spread in an Opposed Forced Flow: The Effect of Ambient Oxygen Concentration, 18th Symposium on Combustion, pp. 579-589 (1981).

[13]Grayson, G., Sacksteder, K.R., Ferkul, P. V., and T'ien, J.S.: Flame Spreading Over a Thin Solid in Low Speed Concurrent Flow: Drop Tower Experimental Results and Comparison with Theory, Microgravity Science and Technology, VII 2: 187 (1994).

[14]Shih, H.-Y. and T'ien, J. S.: Modeling Wall Influence on Solid-Fuel Flame Spread in a Flow Tunnel, presented at the AIAA 35th Aerospace Sciences Meeting, AIAA-97-0236 (1997).

[15]West, J., Tang, L., Altenkirch, R. A., Bhattacharjee, S., Sacksteder, K. R., and Delichatsios, M.A.: Quiescent Flame Spread Over Thick Fuels in Microgravity, 26th Symp. on Comb., pp. 1335-1343 (1997).

[16]Shu, Y., T'ien, J. S., Dietrich, D. L., and Ross, H. D.: Modeling of Candle Flame and Near Extinction Oscillation in Microgravity, Proceedings of the 1st Pan Pacific Conference on Microgravity Sciences (to appear), and Tokyo, Japan (1998).

[17]Olson, S. L., Ferkul, P. V. and T'ien, J. S.: Near-Limit Flame Spread over a Thin Solid Fuel in Microgravity, 22nd Symposium (International) on Combustion, pp. 1213-1222 (1988).

[18]T'ien, J. S.: The Possibility of a Reversal of Material Flammability Ranking from Normal Gravity to Microgravity, Combustion and Flame, Vol. 80 (1990).

[19]Sacksteder, K.R., and T'ien, J.S., "Buoyant Downward Diffusion Flame Spread and Extinction in Partial-Gravity Accelerations," 25th Symposium (International) on Combustion, pp. 1685-1692, (1994).

[20]Lucid, S. W.: Six Months on Mir, Scientific American (May, 1998).

[21]Kimzey, J. H.: Space Experiment M-479: Zero Gravity Flammability, JSC 22293 (1986).

[22]Olson S. L. and Sotos R. G.: Combustion of Velcro in Low Gravity, NASA TM 88970 (1987).

[23]Flammability, Odor, and Offgassing Requirements and Test Procedures for Materials in Environments that Support Combustion, NASA NHB-8060.1C (1991).

[24]Cheatham, S. and Matalon, M.: Near Limit Oscillations of Spherical Diffusion Flames, AIAA Journal, Vol. 34, No. 7, p. 1403 (1996).

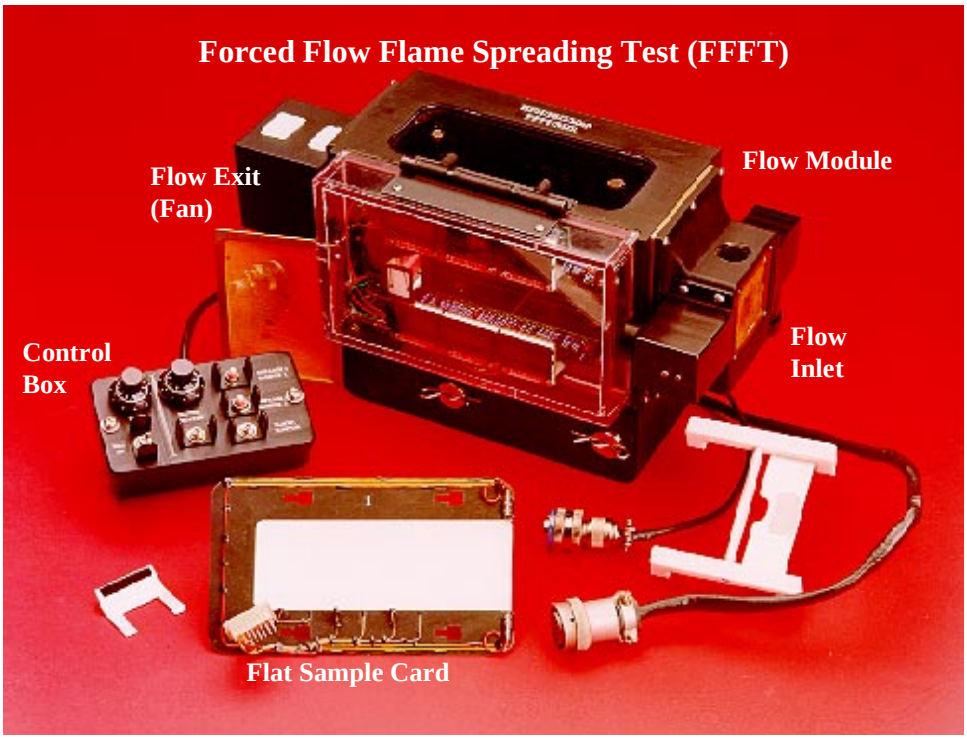

Figure 1. FFFT Hardware

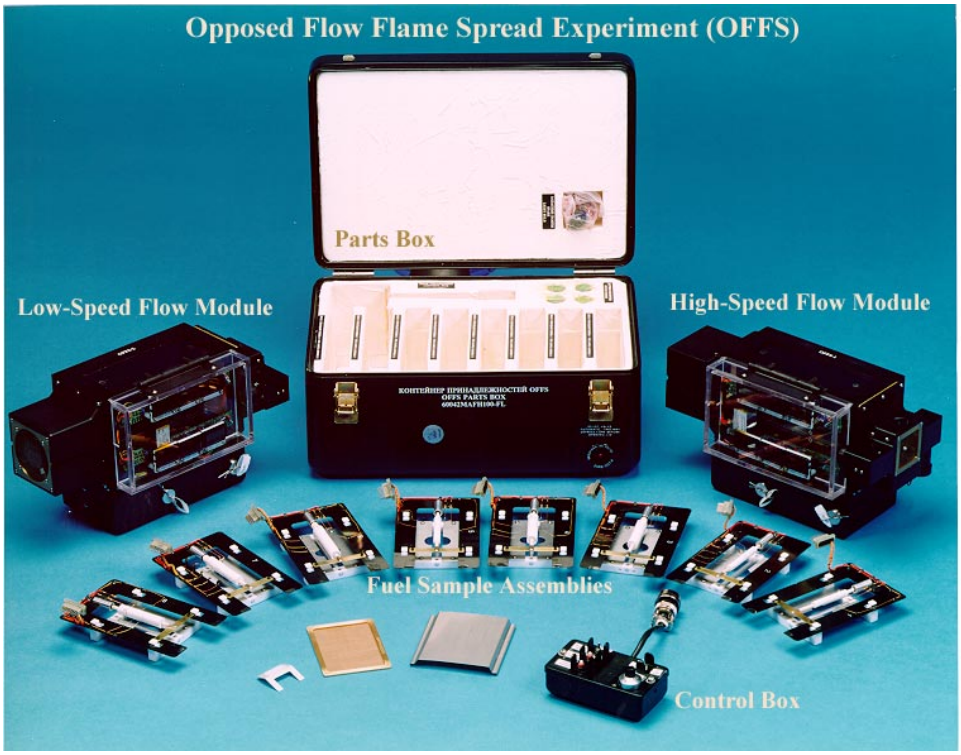

Figure 2. OFFS Hardware

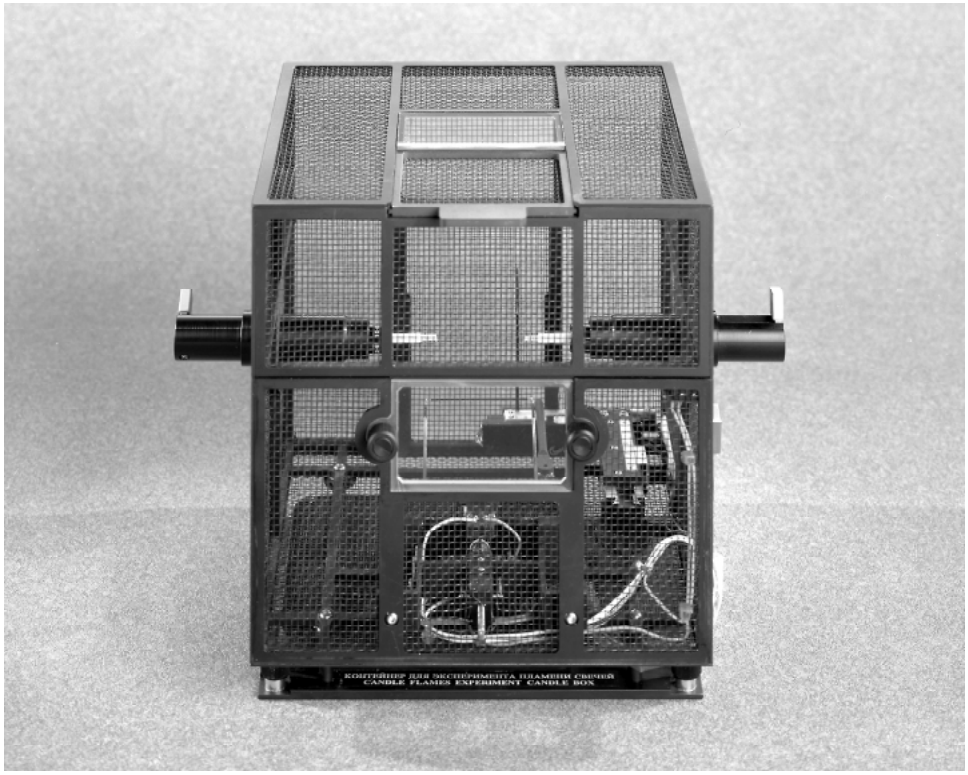

Figure 3. CFM Hardware

Figure 4. Flame Images for Paper Sheets Burning in a Concurrent Flow Speed of 2 cm/s:
From left to right: The area densities are 1, 4, 16, and 40 mg/cm^2 ;
The flame base spread rates are 0.84, 0.089, 0.07, and 0.023 cm/s ;
The flame tip spread rates are 0.58, 0.075, 0.082, and 0.044 cm/s.

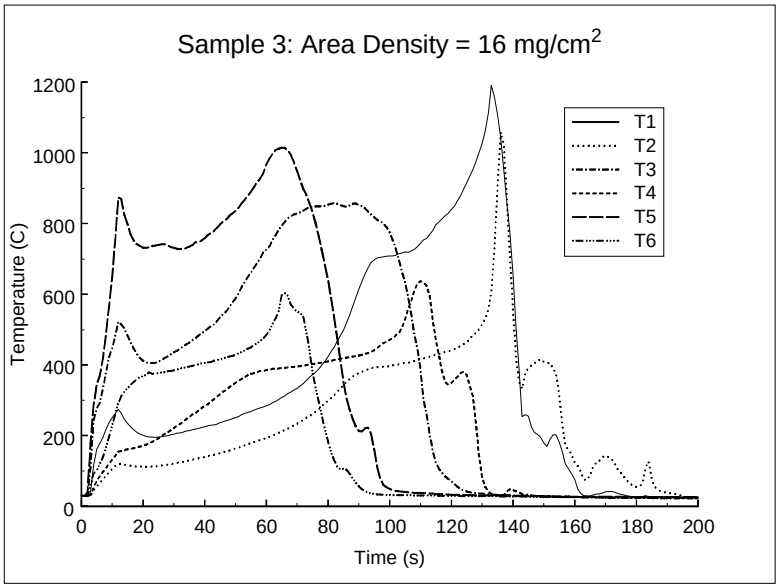

Figure 5. Temperature Traces for Paper Sheet Sample 3.

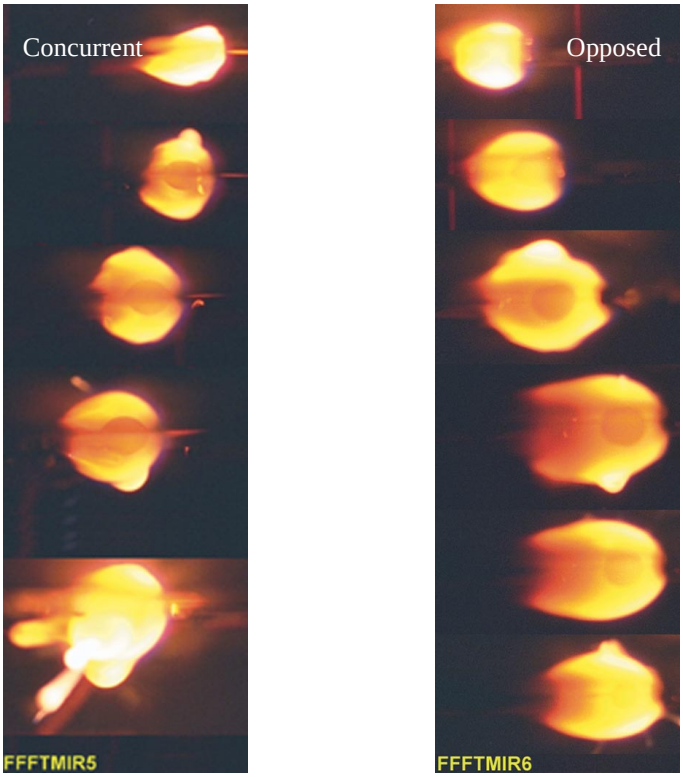

Figure 6. Combustion of Polyethylene Cylinders in Microgravity:
Sequential images are shown from top to bottom; in both cases, the air flow is from right to left.
The concurrent-flow flame spreads at 0.16 cm/s in a 2 cm/s air flow.
The opposed-flow flame spreads at 0.12 cm/s in a 3 cm/s air flow.

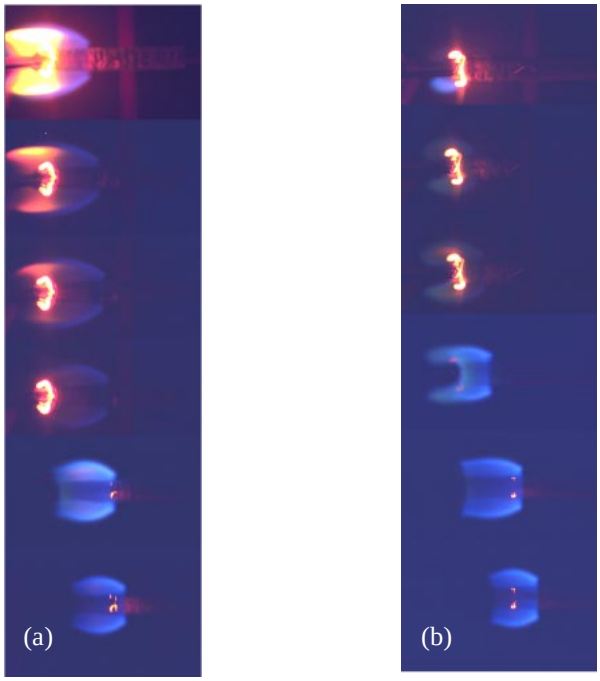

Figure 7. Flames Burning Small-Diameter Cylinders of Cellulose in Opposed Flow.
Sequential images are shown from top to bottom; in both cases, the air flow is from right to left.
a) Flow speed = 5 cm/s; spread rate = 0.16 cm/s
b) Flow speed = 3 cm/s; spread rate = 0.077 cm/s

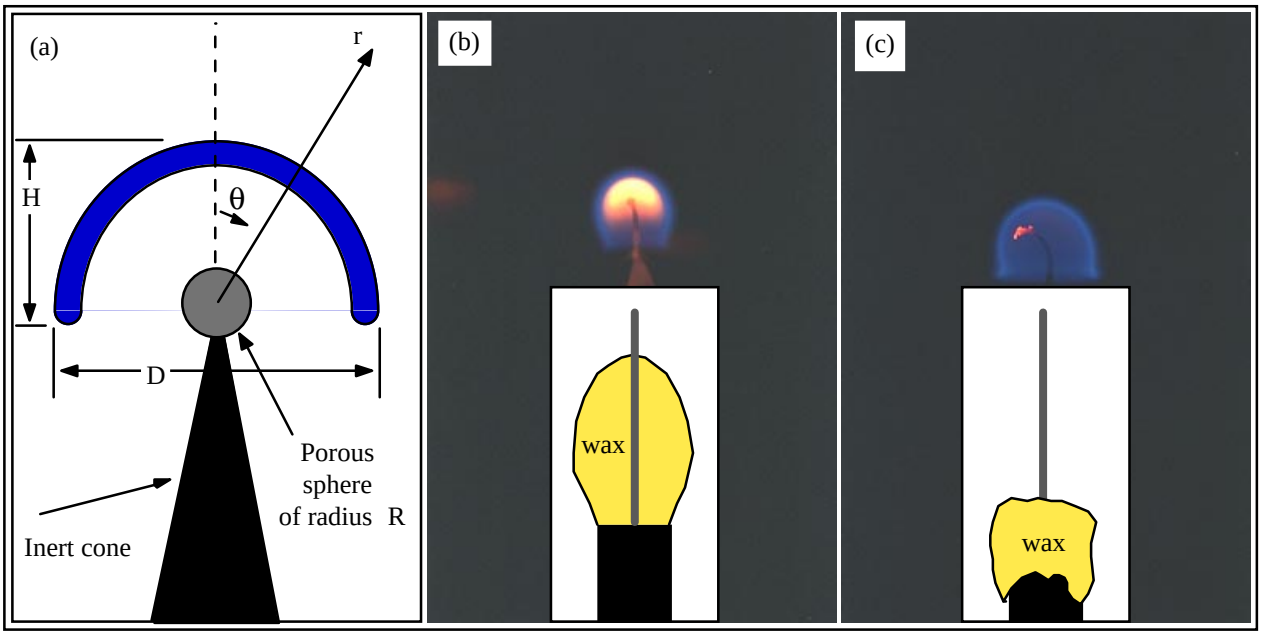

Figure 8. (a) Schematic of a microgravity candle flame with relevant dimensions and coordinate system for numerical model; (b) Candle flame before wax collapse; (c) Candle flame after wax collapse

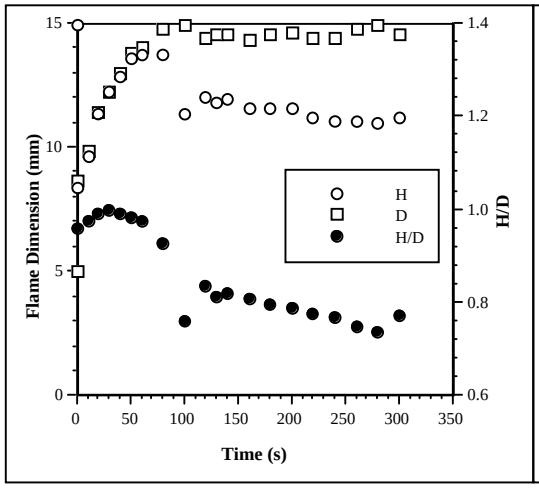

Figure 9. Candle flame height, H, and diameter, D, as a function of time for a candle with a small wick

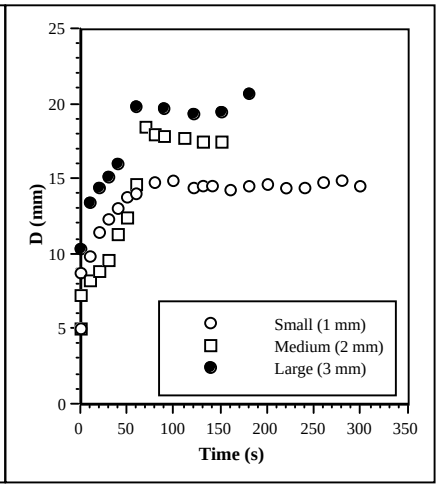

Figure 10. Flame diameter as a function of time for three different wick diameters

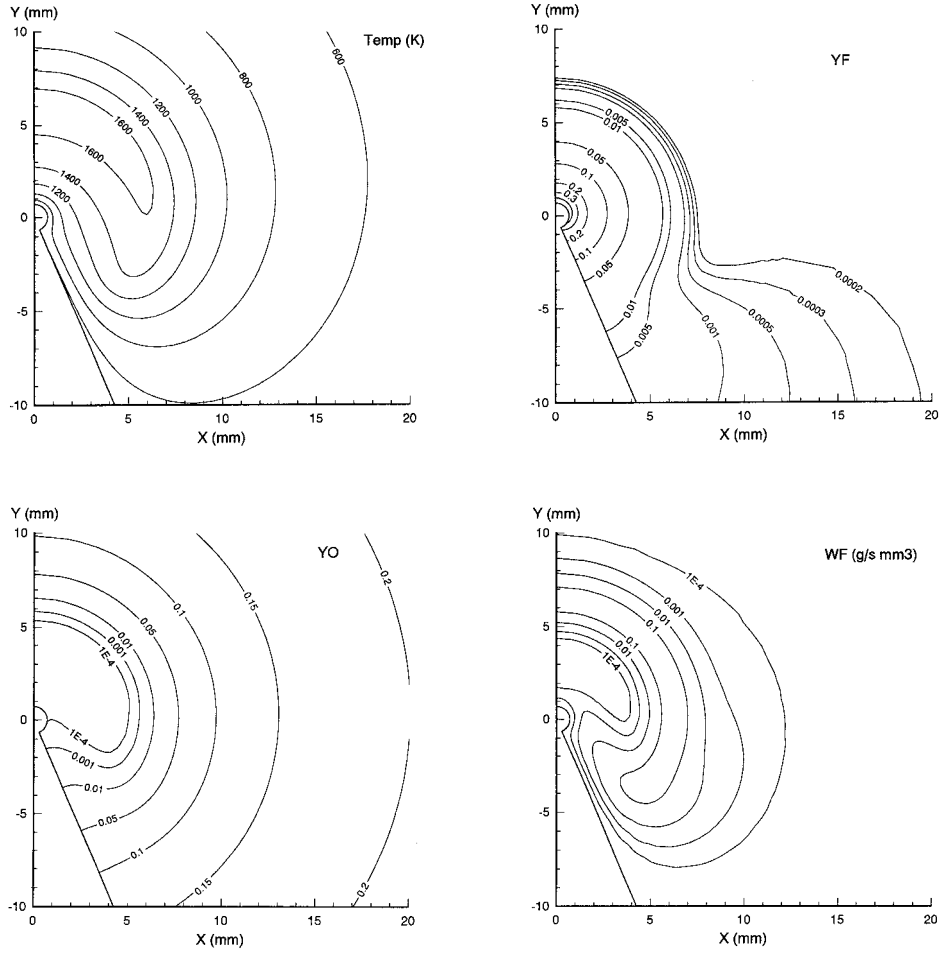

Figure 11. Numerical modeling results for a sphere diameter of 1.2 mm in 1 atm, 23% O_2

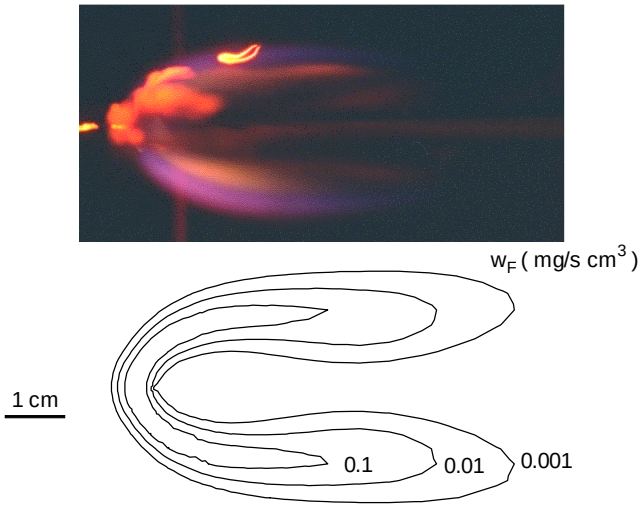

Figure 12. Concurrent-flow combustion of a paper sheet (half-thickness area density = 1.0 mg/cm ^{2}): comparison of visible flame to numerically predicted fuel consumption rate contours. Flow is from left to right at 2 cm/s. Note that the flame is still shrinking in size, while the model results are steady.